INSTITUTE OF PHYSICS PUBLISHING JOURNAL OF PHYSICS: CONDENSED MATTER

J. Phys.: Condens. Matter **13** (2001) 3831–3837 www.iop.org/Journals/cm PII: S0953-8984(01)22171-7

Analysis of the temperature-dependent quantum point contact conductance in relation to the metal–insulator transition in two dimensions

V Senz[1], T Heinzel[1], T Ihn[1], S Lindemann[1], R Held[1], K Ensslin[1], W Wegscheider[2,3] and M Bichler[3]

[1] Solid State Physics Laboratory, ETH Zürich, 8093 Zürich, Switzerland
[2] Walter Schottky Institut, TU München, 85748 Garching, Germany
[3] Institut für Angewandte und Experimentelle Physik, Universität Regensburg, 93040 Regensburg, Germany

Received 20 February 2001, in final form 30 March 2001

Abstract

The temperature dependence of the conductance of a quantum point contact has been measured. The conductance as a function of the Fermi energy shows temperature-independent fixed points, located at roughly multiple integers of e^2/h. Around the first fixed point at e^2/h, the experimental data for different temperatures can be scaled onto a single curve. For pure thermal smearing of the conductance steps, a scaling parameter of one is expected. The measured scaling parameter, however, is significantly larger than 1. The deviations are interpreted as a signature of the potential landscape of the quantum point contact, and of the source–drain bias voltage. We relate our results phenomenologically to the metal–insulator transition in two dimensions.

Conductance quantization in short, quasi-one-dimensional wires [1, 2] ('quantum point contacts'—QPCs) has been widely investigated since its discovery. Meanwhile, QPCs have become key devices in transport experiments in low-dimensional systems [3]. Recently, QPCs have attracted renewed interest in relation to the metal–insulator transition (MIT) in two dimensions [4]: it has been suggested that near the fixed point of the MIT, which typically occurs at a conductance of $G \approx e^2/h$, the carrier gas segregates into conductive puddles [5], which are connected via quantum point contacts [6]. Within such a percolation picture, a statistical ensemble of QPCs determines the transport properties of the inhomogeneous carrier system, since the applied external voltage drops predominantly across the QPCs. Of particular importance is the fixed point in the temperature-dependent conductance of QPCs at e^2/h, which enters in the more general discussion of the quantum percolation model of reference [6] and, within this model, corresponds to the fixed point of the metal–insulator transition in the two-dimensional carrier gas.

This is our motivation for studying in detail the temperature dependence of the conductance of a single QPC, as the elementary unit of such a quantum percolation network, around

0953-8984/01/173831+07$30.00

this fixed point. Theoretically, one expects the conductance $G(\mu, T)$ of a spin-degenerate QPC as a function of the chemical potential μ and the temperature T to be independent of temperature at $G = ne^2/h$, with n being an integer. These fixed points separate regions $(2n-1)e^2/h < G < 2ne^2/h$, in which G decreases as T is increased, from regions $2ne^2/h < G < (2n+1)e^2/h$, where G increases as T is increased.

In a simple picture, $G(\mu, T = 0)$ can be modelled by a sum of step functions. For the fixed point lowest in energy, $n = 1$, we obtain

$$G(\mu, T) = \frac{2e^2}{h} \int \Theta(E - E_1) \left[-\frac{\partial f(E)}{\partial E} \right] \mathrm{d}E = \frac{2e^2}{h} [1 + \mathrm{e}^{(E_1 - \mu)/k_B T}]^{-1}. \quad (1)$$

Here, f is the Fermi function, and E_1 is the energy of the first one-dimensional subband. Furthermore, we have assumed that the voltage drop across the QPC is small compared to $k_B T$. Since within this model, $G(\mu, T)$ has the shape of a Fermi function, the temperature-dependent conductance traces obtained for fixed μ can be scaled onto a single curve $G^*(\delta/T^{1/\alpha})$, with $\delta = (\mu - E_1)/E_1$ and the scaling parameter $\alpha = 1$. G^* consists of two branches, corresponding to the metallic and the insulating regions. Note that here, in contrast to the heavily debated scaling properties of two-dimensional systems [4], scaling does *not* imply a possible quantum phase transition at $T = 0$. Nevertheless, it is interesting in view of reference [6] to compare α obtained here with the scaling parameters found in two-dimensional systems showing a MIT.

The temperature dependence of the conductance quantization in QPCs has been addressed in several experiments [7–15], in particular with respect to the so-called '0.7-feature' [13–15]. To our knowledge, the fixed point at $G = e^2/h$ and the temperature dependence around it has not been investigated yet. However, fixed points have been detected occasionally, while the observed behaviours around these fixed points vary greatly and definitely differ from the expectation expressed by equation (1). Yacoby *et al* [12], for example, observe a fixed point at $G = 1.5e^2/h$ only, around which the metallic and the insulating phases appear reversed. This anomaly probably originates in the observed non-universal conductance quantization. Thomas *et al* [13] observe fixed points at $G = 3e^2/h$ and $G = 2e^2/h$, but not at $G = e^2/h$, which is possibly destroyed by the 0.7-feature.

In the present paper, we report the observation of a series of clear fixed points ($n = 1, \ldots, 5$) in a QPC. We investigate $G(\mu, T)$ around the fixed point at $G \approx e^2/h$ in further detail. $G(\mu, T)$ can be scaled reasonably well onto a single curve. The scaling parameter α, however, is significantly larger than 1 (the value assumed in reference [6]), and increases monotonically as the source–drain bias voltage is increased. Possible implications for describing the MIT in two dimensions in terms of a quantum percolation model are discussed.

The sample is a Ga[Al]As heterostructure, grown by molecular beam epitaxy, with the 2DEG 34 nm below the surface. The QPC is defined by local oxidation with an atomic force microscope [16] (insets in figure 1). The lithographic channel width is 80 nm, and its length is given by the width of the oxide lines, i.e., 140 nm. The QPC can be tuned by voltages applied to a homogeneous top gate (tg) and to the planar gate (pg). A top-gate voltage changes μ throughout the sample. However, G is still governed by the QPC, and the effect of the top gate on the surrounding 2DEG is negligible, as long as it is not depleted. The sample is mounted in a ^{4}He cryostat, in which the temperature can be varied between 1.7 K and room temperature, or in the mixing chamber of a ^{3}He/^{4}He dilution refrigerator with a base temperature of 90 mK, respectively. The electron density of the ungated 2DEG is 5.5×10^{15} m^{-2}, and the mobility of the 2DEG is 93 m^2 V^{-1} s^{-1} at $T = 4.2$ K.

AC resistance measurements are performed in a four-terminal set-up. As the top-gate voltage V_{tg} or the temperature is changed, the voltage drop V_b across the QPC is kept constant by

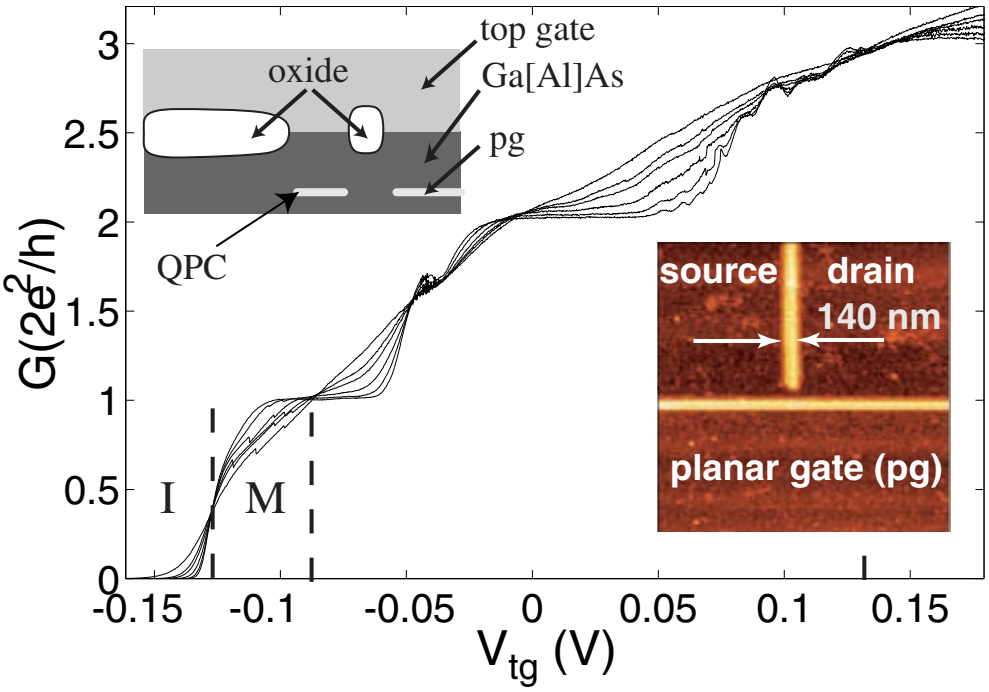

Figure 1. The lower right inset shows the surface topography of the sample, measured with an AFM directly after the oxidation step. The QPC is defined by two oxide lines (bright lines), and connects source with drain. Upper left inset: cross section through the device, after deposition of the top gate, along a vertical line through the QPC in the lower inset. Below the oxide lines, the 2DEG is depleted. Main figure: conductance G as a function of the top gate voltage, taken at temperatures of 1.7 K, 5 K, 8 K, 12 K, 15 K, and 20 K. The metallic and insulating regions around $G = e^2/h$ are indicated by 'M' and 'I'. Here, the planar gate voltage was -100 mV, and $V_b = 50\ \mu$V.

(This figure is in colour only in the electronic version, see `www.iop.org`)

a feedback loop which adjusts the current accordingly. This constant voltage drop is important, since V_b modifies $G(\mu, T)$, as will be discussed below. Figure 1 shows G as a function of V_{tg} for different temperatures. The conductance quantization has a characteristic temperature of $\approx$15 K, which corresponds to an energy separation between the one-dimensional subbands of $\hbar\omega_y = 3.52 k_B T \approx 4.5$ meV. Here, ω_y denotes, within a parabolic approximation, the confining strength transverse to the transport direction. Fixed points occur at roughly multiple integers of e^2/h, and separate metallic regions from insulating regions.

The traces contain additional conductance fluctuations between the plateaus, which depend on the cooling cycle, but are always present and perfectly reproducible within one cooling. They are probably due to imperfect adiabatic coupling between the QPC and the reservoirs, or due to nearby scatterers. At temperatures below 1 K, the shapes of the steps are independent of temperature (not shown), indicating that the smearing of the steps is not solely determined by temperature.

We therefore model the QPC potential by a parabolic saddle-point potential [17], i.e.

$$V(x, y) = V_0 - \frac{1}{2} m^* \omega_x x^2 + \frac{1}{2} m^* \omega_y^2 y^2.$$

V_0 is the potential energy of the saddle point, m^* the effective electron mass, and ω_x denotes the

curvature of the saddle-point potential in the transport direction. Using this model is justified since, in the following, we focus on the regime $G < 2e^2/h$.

The transmission $T(\epsilon)$ for the lowest one-dimensional subband can be written as [17]

$$T(\epsilon) = [1 + \mathrm{e}^{-\pi\epsilon}]^{-1} \qquad \epsilon = 2\left(E - \frac{1}{2}\hbar\omega_y - V_0\right)\Big/\hbar\omega_x. \tag{2}$$

Here, E denotes the energy of the incident electrons. Since the separation of the conductance plateaus corresponds to $\hbar\omega_y$ in energy, we can estimate the lever arm inside the QPC and in the regime of the first conductance step using $\mathrm{d}E_F/\mathrm{d}V_{tg} \approx 50$ meV V^{-1}, which we use to transform V_{tg} into energy. In the limit of $V_b = 0$ and for negligible temperatures, the width of the step edge corresponds to $\hbar\omega_x$. Hence, we can estimate $\hbar\omega_x \approx 2$ meV from figure 1.

We proceed by studying the 'metal–insulator transition' around $G = e^2/h$ in more detail (figure 2).

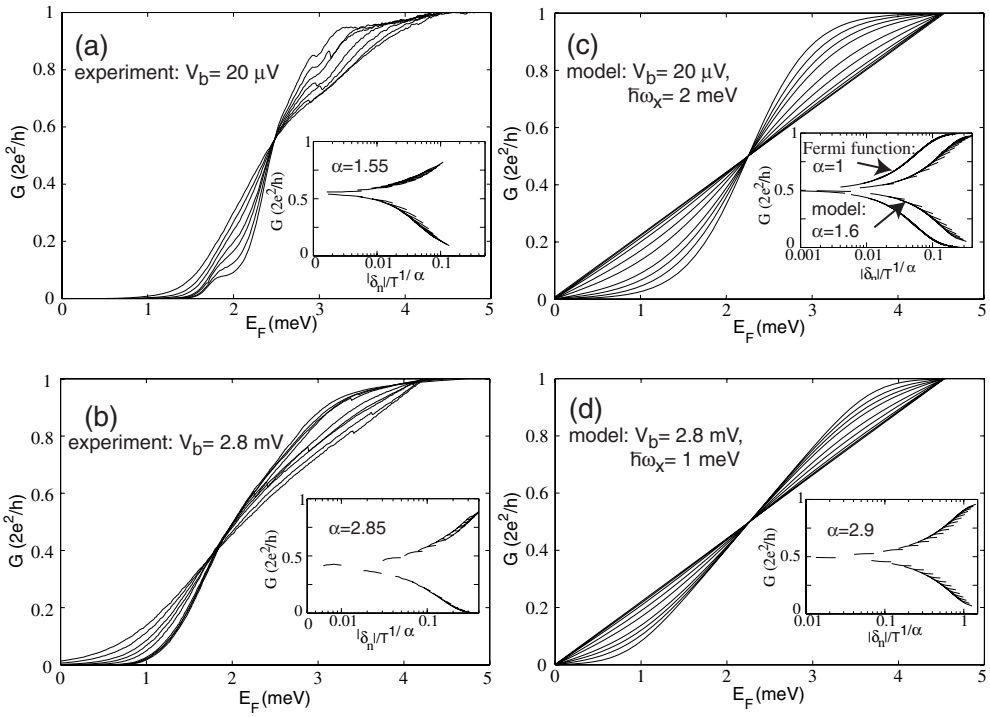

Figure 2. Conductance of the QPC as a function of the Fermi energy, as measured for $V_{sd} = 20\,\mu$V (a) and for $V_{sd} = 2.8$ mV (b). The Fermi energy was calculated from V_{tg} using the lever arm (see the text). The insets show the corresponding scaling plots and the scaling parameters obtained. In (c) and (d), the calculated conductances within the model described in the text for the corresponding V_{sd} are shown, together with the scaling functions of the calculated conductance traces. In addition, in the inset in (c), the scaled thermally smeared Fermi function is shown for comparison, which has $\alpha = 1$.

As V_b is increased, the fixed point remains well defined and shifts to smaller conductances. In addition, the step edge broadens significantly. In the insets of figures 2(a) and 2(b), we show the best scaling achieved with the scaling variable $|\delta|/T^{\alpha}$, using α as a parameter. Scaling of the experimental data works well, although less well than for many two-dimensional systems showing a MIT [18]. The scaling parameter α, however, is larger than 1 and increases as V_b is increased. We estimate the error of α to be $\delta\alpha \approx \pm 0.3$ at small V_b, which increases for

higher bias voltages. Thus, the MIT is clearly *not* solely determined by thermal smearing, as equation (1) suggests.

In order to understand the origin of the step edge slope and the experimental scaling parameter in more detail, we consider a simple model, which includes thermal smearing, the potential landscape in the transport direction, described by ω_x, and the bias voltage V_b. We therefore follow reference [7] and model the current I by

$$I = \frac{e}{\pi\hbar}\int T(\epsilon)[f(E-(E_F+eV_b),T)-f(E-E_F,T)]\,\mathrm{d}E \tag{3}$$

where $T(\epsilon)$ is given by equation (2), and use ω_x as a parameter in order to obtain agreement with the experiment (figures 2(c) and 2(d)). With equation (3), we can describe the experimental results, provided that we allow ω_x to decrease as V_b is increased. Such an effect is quite reasonable, since the potential drop in the transport direction is superimposed on the saddle-point potential, which may result in a reduction of the curvature ω_x at the saddle point. Furthermore, we have assumed in the model that ω_y is independent of V_b, as observed experimentally, i.e. the separation of the steps in V_{tg} does not depend on V_b. Also, our model does not make any assumptions on how the voltage drops along the QPC [19].

The conductance traces obtained from equation (3) no longer scale exactly onto a single curve (figures 2(c) and 2(d)). However, the scaling analysis not only allows us to express the behaviour around the fixed point in terms of a single parameter, but also shows that the imperfect scaling of the experimental data can be expected from models differing from the oversimplified one described by equation (1).

The insets in figure 2 show the scaled data (scaling functions) of the main figures. As V_b increases, ω_x has to be reduced in order to obtain agreement between the scaling parameters in the experiment and in the model. This behaviour is more clearly shown in figure 3, where we plot the results of many simulations and compare them with the experimental data.

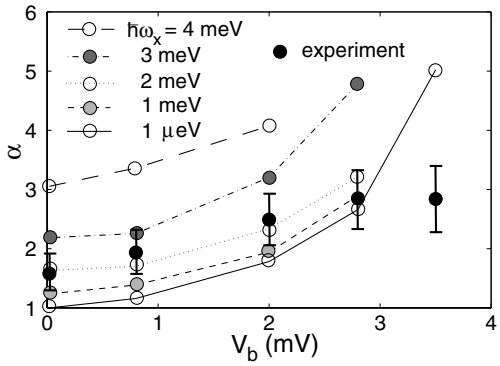

Figure 3. Comparison between the experimentally obtained values for α (full circles) and those obtained for various values of ω_x (see the key) within our model. The model predicts a scaling parameter increasing as V_{sd} increases, which is also seen in the experiment. For $V_b \leqslant 2$ mV, the experimental values of α agree well with the model, assuming $\hbar\omega_x \approx 2$ meV. For $V_b > 2$ mV, deviations occur (see the text).

It can be seen that for $eV_b \geqslant \hbar\omega_x$, the ω_x needed in the simulation in order to reproduce the experimental scaling parameter becomes smaller. The reason for this is possibly again the simplifications made in our model, or nonlinearities in the current–voltage characteristics, which are expected as soon as eV_b becomes of the order of the subband spacing $\hbar\omega_y$. For small source–drain bias voltages, however, the experimentally obtained scaling parameter can be interpreted as a measure of ω_x.

The model developed by Meir in reference [6] describes the recently observed MIT in two dimensions in terms of a network of quantum point contacts with statistically distributed conductances. This network can be thought of as being composed of two characteristic conductances, a metallic one (σ_m) and an insulating one (σ_i), which determine the scaling behaviour of the network around the percolation threshold. Thus, this model cannot be applied to the MIT at a *single* QPC, as investigated in our experiment. Nevertheless, our results are related to Meir's model, since they demonstrate that the shape of the saddle potential influences σ_m and σ_i. Within a simple approximation, however, a connection between the MIT on a QPC and that in a disordered two-dimensional carrier gas can be made. In the case of a disordered system consisting of conductive puddles, connected by *identical* QPCs, the scaling parameter obtained experimentally from scaling the MIT of the disordered system is directly related to ω_x. It is the characterizing parameter for the connections between the puddles (note that within our simple model, the macroscopic voltage drop measured corresponds to the voltage drop across a single QPC, except for a geometry factor).

The samples which perhaps come closest to such a scenario are those studied by Ribeiro *et al* [20]. There, self-assembled quantum dots are embedded in the plane of the electron gas. The dots, which act as repulsive scatterers, have a diameter of only 30 nm, a separation of $\approx$80 nm on average, and are very homogeneous in size. It is thus quite possible that between the self-assembled dots, QPCs are formed, in which only the lowest subband is occupied. Analysing the MIT observed in these disordered samples gives $\alpha = 2.6$ at small bias voltages [20], which, within our model, corresponds to a realistic value of $\hbar\omega_x \approx 3.5$ meV.

In summary, we have observed a sequence of fixed points in a single quantum point contact. The scaling behaviour of the temperature-dependent conductance around the fixed point in the lowest subband has been studied, and significant deviations from simple Fermi function scaling have been found. Besides temperature, the scaling parameter is also determined by the potential shape of the QPC in the transport direction, which we have quantified by the curvature ω_x, and by the source–drain voltage. Our experiment and analysis suggest that in order to further check the validity of Meir's model, an artificial, random network of quantum point contacts should be studied.

Acknowledgments

Financial support by the Schweizerischer Nationalfonds is gratefully acknowledged.

References

[1] van Wees B J, van Houten H, Beenakker C W J, Williamson J G, Kouwenhoven L P, van der Marel D and Foxon C T 1988 *Phys. Rev. Lett.* **60** 848

[2] Wharam D A, Thornton T J, Newbury R, Pepper M, Ahmed H, Frost J E F, Hasko D G, Peacock D C, Ritchie D A and Jones G A C 1988 *J. Phys. C: Solid State Phys.* **21** L209

[3] For a review, see
van Houten H, Beenakker C W J and van Wees B J 1992 Quantum point contacts *Semiconductors and Semimetals* vol 35 (San Diego, CA: Academic) ch 2

[4] Kravchenko S V, Kravchenko G V, Furneaux J E, Pudalov V M and D'Iorio M 1994 *Phys. Rev.* B **50** 8039
For a recent theoretical discussion, see
Altshuler B L, Maslov D L and Pudalov V M 2000 *Preprint* cond-mat/0003032

[5] The formation of such puddles has recently been verified experimentally by near-field photoluminescence:
Eytan G, Yayon Y, Rappaport M, Shtrikman H and Bar-Joseph I 1998 *Phys. Rev. Lett.* **81** 1666
as well as by local capacitance spectroscopy:
Ilani S, Yacoby A, Mahalu D and Shtrikman H 2000 *Phys. Rev. Lett.* **84** 3133

[6] Meir Y 1999 *Phys. Rev. Lett.* **83** 3506
Meir Y 2000 *Phys. Rev.* B **61** 16 470
[7] Bagwell P F and Orlando T P 1989 *Phys. Rev.* B **40** 1456
[8] van Wees B J, Kouwenhoven L P, Willems E M M, Harmans C J P M, Mooij J E, van Houten H, Beenakker C W J, Williamson J G and Foxon C T 1989 *Phys. Rev.* B **43** 12 431
[9] Frost J E F, Simmons M Y, Pepper M, Churchill A C, Ritchie D A and Jones G A C 1993 *J. Phys.: Condens. Matter* **5** L559
[10] Dzurak A S, Smith C G, Martin-Moreno L, Pepper M, Ritchie D A, Jones G A C and Hasko D G 1993 *J. Phys.: Condens. Matter* **5** 8055
[11] Taboryski R, Kristensen A, Sorensen C B and Lindelof P E 1995 *Phys. Rev.* B **51** 2282
[12] Yacoby A, Stormer H L, Wingreen N S, Pfeiffer L N, Baldwin K W and West K W 1996 *Phys. Rev. Lett.* **77** 4612
[13] Thomas K J, Nicholls J T, Simmons M Y, Pepper M, Mace D R and Ritchie D A 1996 *Phys. Rev. Lett.* **77** 135
[14] Thomas K J, Nicholls J T, Appleyard N J, Simmons M Y, Pepper M, Mace D R, Tribe W R and Ritchie D A 1998 *Phys. Rev.* B **58** 4846 and references therein
[15] Kristensen A, Bruus H, Hansen A E, Jensen J B, Lindelof P E, Marckmann C J, Nygård J, Sørensen C B, Beuscher F, Forchel A and Michel M 2000 *Phys. Rev.* B **62** 10 950
[16] Held R, Vancura T, Heinzel T, Ensslin K, Holland M and Wegscheider W 1998 *Appl. Phys. Lett.* **73** 262
[17] Büttiker M 1990 *Phys. Rev.* B **41** R7906
[18] For a list of references, see
Senz V, Heinzel T, Ihn T, Ensslin K, Dehlinger G, Grützmacher D and Gennser U 2000 *Phys. Rev.* B **61** R5082
[19] Ulreich S and Zwerger W 1998 *Superlatt. Microstruct.* **23** 719
[20] Ribeiro E, Jäggi R D, Heinzel T, Ensslin K, Medeiros-Ribeiro G and Petroff P M 1999 *Phys. Rev. Lett.* **82** 996